International Journal of Chemical and Biochemical Sciences
(ISSN 2226-9614)

Journal Home page: www.iscientific.org/Journal.html

The synergistic inhibitive effect of *Agave americana* and iodide ions on the sulfuric acid corrosion of mild steel

***Sameh. Athmani*[1, 2]* *and Sihem. Abderrahmane*[1]**

[1]*Laboratory of Engineering Surfaces, Badji Mokhtar-Annaba University, Annaba, Algeria and* [2]*Center for Scientific and Technical Research in Physico-Chemical Analyzes. BP 384, Bou-Ismail, RP 42415 Tipaza, Algeria*

Abstract

The synergistic effect of *Agave americana* Extract (AAE) with KI on mild steel corrosion inhibition in 0.5 M H_2SO_4, was investigated by Electrochemical Impedance Spectroscopy (EIS), Potentiodynamic Polarization (PDP) and Potential Zero Charge (PZC) methods, as well as the effect of temperature. The AAE composition and the adsorbed film were analyzed by Attenuated Total Reflection - Fourier-Transforms Infrared Spectroscopy (ATR-FTIR) and Scanning Electron Microscope (SEM). The results obtained showed that the presence of synergy increased the inhibition efficiency to 86.24 %. The synergism parameter indicating a competitive adsorption. Inhibition efficiency decreased with increase in temperature from 298 K to 308 K but increased at relatively high temperature of 328 K. The activation energy, enthalpy and entropy results indicated that the adsorption mechanism was of chemical nature.

Keywords: Corrosion, Inhibitor, Agave Americana Extract, Synergistic effect, Sulfuric acid

Full length article **Corresponding Author*, e-mail: samehathmani@yahoo.fr

1. Introduction

The synergistic effect plays an essential role in improving inhibition efficiency, reducing the inhibitor amount and diversifying its applications in different media [1, 2]. The A37 steel corrosion in 0.5 M NaCl was studied by Ouchenane *et al.* [3]. The obtained inhibition efficacy was 48 % using 20 ppm HEDP alone, while the synergy of 10 ppm HEDP + 200 ppm Y^{+3} increased the inhibition efficacy 75 %. Bahlakeh *et al.* [4], confirmed that during mild steel corrosion in chloride solution, the combination of 200 ppm's *Nettle* leaves extract and 200 ppm's zinc salt increased the inhibition efficiency 61 % and 77 %, respectively for each single compound to 98 % in the case of their synergy.

Among the anions group, the halide ions are the most used, several research works investigated the synergistic effect. The study of copper corrosion's inhibition in 1 M HNO_3 by 10^{-4} M *L-methionine* alone reached 95.75 % inhibition efficiency which increased to 98 %, during the synergy of 10^{-4} M *L-methionine* and 10^{-3} M KI [5].The effect of *Nypa fruticans'wurmb* extract on mild steel corrosion in 0.1 M HCl gave 77.31% inhibition efficiency raising to 95.36 % by 0.05 M KI at 30 ˚C addition [6]. The study of aluminum corrosion inhibition by *Aningeria robusta* extract in 2 M HCl, was studied by Obot *et al.* [7]. They obtained 65 % inhibition efficiency for 50 % (v/v) of the extract at 30 ˚C. The addition of 5 mM KI has enhanced the inhibition efficiency to 90 %. The studies conducted by Jokar *et al.* [8] on carbon steel corrosion's inhibition in 1M HCl by *Morus alba* Pendula extract leaves (MAPLE), achieved 93 % efficiency for 0.4 g/L of MAPLE at 25°C. The addition of 10 mM KI augmented the inhibition efficiency to 96 %.

The halide ions' addition to corrosive medium increases the adsorption capacity of the inhibitor's organic cations, which allowed the iodide ion to form a bridge between theme and metal surface. It is reported in the literature that the iodide ion's effect during a synergy is better compared to the other halides, due to its large ionic radius (135 pm), high hydrophobicity, and atomic mass [9-11].

This work is performed to the synergistic effect's study (2000 ppm *Agave americana* Extract (AAE) and 10^{-3} M KI), for the mild steel (MS) corrosion's inhibition in 0.5 M H_2SO_4. For that, the transitory electrochemical methods (EIS), stationary potentiodynamic curves, the zero charge potential method and the temperature effect, have been evaluated in order to obtain the inhibition efficiency.

2. Experimental

2.1. Preparation of Agave americana extract

The *Agave americana* (AA) plant used in our work grows in Algerian coast (Annaba). It was cleaned with distilled water and then cut into small pieces and then placed in a soxhlet. Methanol was chosen as an extraction solvent. After six hours, a mixture of solvent and liquid form plant extract was recuperated and placed into a rotary evaporator to obtain a solid extract called Agave Americana Extract (AAE).

2.2. Materials and solutions

The composition (wt.%) of mild steel (MS) sample used in this study is as follows: C 0.17 %; Si 0.59 %; Mn 1.60 %; P 0.04 % and balance Fe. The steel is cut in cylindrical form with 0.5 cm^2 exposed surface area were used as working electrode for polarization and EIS measurements. Prior to the experiments, the samples were mechanically abraded with (320 to 2000 µm) grade of emery papers. It was then degreased with ethanol, washed with distilled water and dried in air before immersing in the corrosive medium.

The corrosive medium is a 0.5 M sulfuric acid solution, obtained by the dilution of 98 % H_2SO_4 (Sigma-Aldrich). The optimum concentration of AAE used was 2000 ppm [12]. Potassium iodide (KI) (Sigma-Aldrich) was used at a concentration of 10^{-3} M. All experiments were carried out at 25 ˚C, controlled by a thermostatic bath and without stirring, in a volume of 100 mL.

2.3. Electrochemical measurements

The experimental device is GAMRY Interface 1000 Potentiostat/Galvanostat assisted by a computer using Gamry Echem Analyst software, connected to a conventional three electrode cell consisting of an Ag/AgCl reference electrode, a platinum auxiliary electrode with 1 cm^2 plate and a 0.5 cm^2 study steel working electrode.

For electrochemical impedance measurements, the scanning was performed from high frequency 100 kHz to low frequency 10 mHz with a sinusoidal perturbation of 5 mV per decade. For potentiodynamic measurements, the anode branches were obtained by conducting a potential scanning from open circuit potential (E_{ocp}) to+0.100V/$_{(Ag/AgCl)}$with 1mV/s scanning rate. The cathodic branches were recorded with the same scanning rate in a potential range from E_{ocp} to -1.00 V/$_{(Ag\ /AgCl)}$.

2.4. Morphological characterization

2.4.1. FTIR spectroscopy

Structural characterization of *Agave americana* extract was performed by ATR-FTIR. The adsorbed inhibition films, at first time obtained in 0.5 M H_2SO_4 + 2000 ppm AAE and, at a second time in 0.5 M H_2SO_4 + 2000 ppm AAE + 10^{-3} M KI after 1 hour of immersion were made by BRUKER Fourier Alpha transform's spectrometer instrument controlled by Opus 6.5 software. This device is equipped with Crystal Attenuated total Reflectance (ATR) accessory made of robust diamond crystal.

2.4.2. Scanning electron microscopy

Scanning Electron Microscopy (SEM) micrographs obtained in different media namely 0.5 M H_2SO_4, 0.5 M H_2SO_4 + 2000 ppm AAE and 0.5 M H_2SO_4 + 2000 ppm AAE + 10^{-3} M KI resulted after 1 hour of immersion, using a Quanta 250 Scanning Electron Microscope with Tungsten Filament.

3. Results and discussions

3.1. Electrochemical impedance spectroscopy

Figure 1 shows the electrochemical impedance diagrams in Nyquist representation of MS in different media. According to Figure 1, the diagrams (2), (3) and (4) consist of a single capacitive loop, whose largest size is attributed to the synergy (2000 ppm AAE + 10^{-3}M KI), while the diagram (1) represents an inductive loop. The electrochemical parameters deduced from the equivalent circuit in Figure 2and after adjustment are given in Table 1. The results show an increase in Rp from 679 to 877 Ω.cm^2, a decrease in CPE_{dl} from 102 to 63 µF.cm^2 and an increase in the inhibition efficiency 76.58% to 81.87% corresponding respectively to 2000 ppm AAE and the synergy (2000 ppm AAE + 10^{-3}M KI)[13,14].

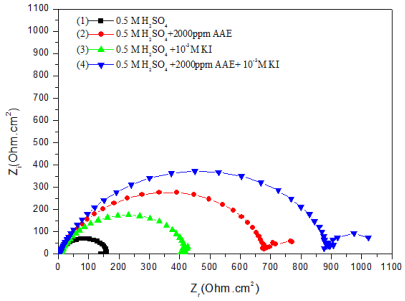

Figure1: Nyquist diagrams of MS in (1) 0.5 M H_2SO_4, (2) 0.5 M H_2SO_4 + 2000 ppm AAE, (3) 0.5 M H_2SO_4 +10^{-3}M KI and (4) 0.5 M H_2SO_4+2000 ppm AAE + 10^{-3}M KI

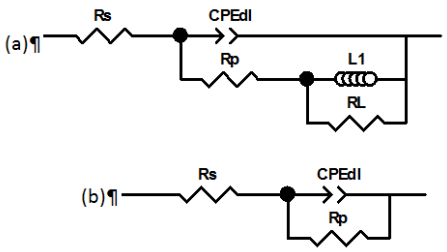

Figure 2: Equivalent electric circuits of MS in 0.5M H_2SO_4 (a) and with AAE, KI and their synergy (b)

3.2. Potentiodynamic polarization

Figure 3 shows the polarization curves of MS in different media. The electrochemical parameters deduced from these curves are represented in Table 2.

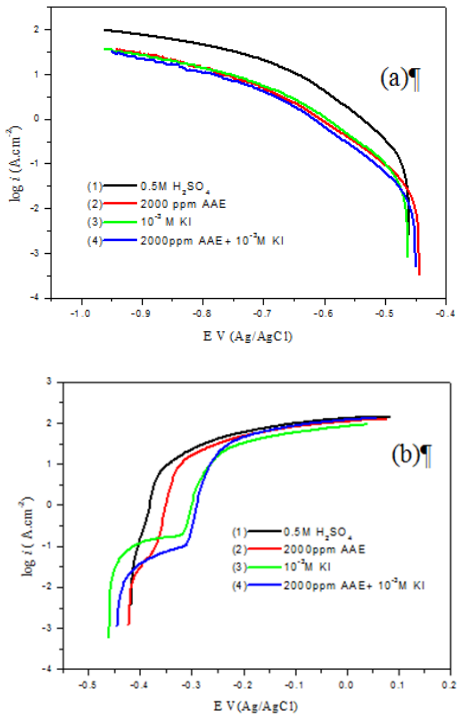

Figure 3: Cathodic (a) and anodic (b) polarization curves of MS in 0.5M de H_2SO_4 (1) with 2000ppm AAE (2), 10^{-3}M KI (3) and 2000ppm AAE +10^{-3}M KI (4)

From Figure 3 (a) representing the cathodic branches, the corrosion potential shifting towards all combinations' positive values namely (2), (3) and (4) corresponding respectively to 2000 ppm AAE, 10^{-3} M KI and 2000 ppm AAE + 10^{-3}M KI compared to curve (1), as well as current density decrease of all the above-mentioned combinations in comparison to the one without inhibitor. According to the Figure 3(b), the anodic branches of the curves (3) and (4), respectively corresponding to 10^{-3} M KI and 2000 ppm AAE + 10^{-3} M KI have the same appearance with the passivation plateau's apparition from [-420 to -320] $mV/_{Ag/AgCl}$, whereas for the curve with AAE 2000 ppm alone, a small passivation level is observed from [-400 to -425] $mV/_{Ag\ /AgCl}$ which denotes that synergy has a beneficial effect on the passivation stage's width due to the formation of protector film on metal surface. Beyond the potential (-225 $mV/_{Ag/AgCl}$). It be observed that all curves are mingled, leading us to conclude that the desorption rate of the inhibiting film is higher than its adsorption rate [15-17].

According to the results obtained in Table 2, the synergy (2000 ppm AAE + 10^{-3} M KI), decreases the corrosion potential from -461.7 to -449.6 $mV/_{Ag/AgCl}$ and the current density from 628.70 at 86.53 $\mu A.cm^{-2}$, which led to inhibition efficiency's increase from 81.87 % to 86.24 % obtained respectively in 2000 ppm AAE alone and 2000 ppm AAE + 10^{-3} M KI. This shows the effect of KI as additive.

3.3. Mechanism of action of AAE by the PZC method

The corrosion inhibition mechanism consists of the inhibitory molecules' adsorption on metal surface. The adsorption process is influenced by nature, metal charge, inhibitor's chemical structure and electrolyte type. Metal surface's charge can be defined by the position of the corrosion potential E_{ocp} with respect to the E_{PZC} [18].

The potential value of Antropov (E_r) is calculated by the following relation:

$$E_r = E_{OCP} - E_{PZC} \quad (E1)$$

If, $E_r < 0$ the electrode surface is negatively charged, which favors the cations' adsorption.

And if, $E_r > 0$, the electrode surface is positively charged, which favors the anions' adsorption.

Figure4 represents a parabola with a maximum (E_{PZC}= -347$mV/_{Ag/AgCl}$) and the abundant potential (E_{ocp}= -447$mV/_{Ag/AgCl}$) of MS in 0.5 M H_2SO_4 with 2000ppm AAE + 10^{-3}M KI. From the obtained value of the Antropov potential (E_r = -100 $mV/_{Ag\ /\ AgCl}$), this conclude that the surface is negatively charged, indicating that the negatively charged iodide ions are adsorbed on the surface of the steel. This result can be interpreted by the following mechanism: The sulphate ions (SO_4^{-2}) being adsorbed, giving a negatively charged surface A.

$AARH^+$ cations, obtained according to reaction 2, are adsorbed on surface A by electrostatic attraction (positively charged surface) (surface B).

$$\mathbf{AAE + H^+ \leftrightarrows AAEH^+} \quad \mathbf{(R2)}$$

The iodide ions, from the KI added to the acid solution containing the cations ($AARH^+$), are chemisorbed on the surface B to obtain a surface C (negatively charged). Similar results were reported [16].

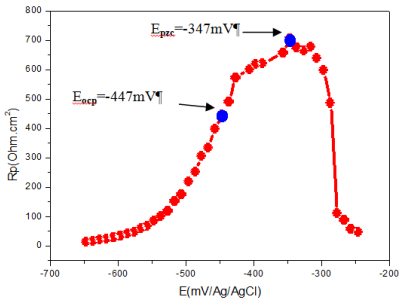

Figure 4: Polarization resistance's variation according to MS potential in 0.5M H_2SO_4 + 2000ppm AAE+10^{-3}M KI

3.4. Synergy parameter(s)

The interaction between AAE molecules and iodide ions can be described by calculating the synergy parameter (s), which is defined as follows:

$$\mathbf{s = \frac{1 - (\theta 1 + \theta 2) - (\theta 1.\theta 2)}{1 - \theta'(1 + 2)}} \ldots \mathbf{(E3)}$$

Where θ1 is the iodide ion surface's recovery rate, θ2 the AAE surface's recovery rate at 2000ppm and θ′(1+2) synergy surface's recovery rate.

For the value of the synergism parameter (S), if S > 1, it manifests synergism in coopérative adsorption and if S < 1, it shows antagonism which may result in competitive adsorption [19] where, one of the compounds is chemisorbed on metal surface and the other is physisorbed on the first.

The synergy parameter (s) calculated from polarization curves' obtained results is shown in Table 2, according obtained value (s = 0.40), we can conclude that there is a competitive synergy.

3.5. Temperature effect and thermodynamic parameters

3.5.1. Temperature effect

Temperature influence ,on the synergy's inhibition efficacy of AAE +10^{-3}M KI on MS in 0.5 M H_2SO_4, was investigated using potentiodynamic polarization at the temperatures 298; 308; 318 and 328 K. Cathodic and anodic polarization curves without and with 2000ppm AAE+10^{-3}M KI at different temperatures are represented in Figure5 and Figure6 respectively. It is noticed the current density rises with temperature increasing (Figure5.(a) and Figure5.(b)).Whereas in synergy presence (2000ppm AAE + 10^{-3}M KI) (Figure6), it is also noticed that the temperature increase causes an increase of corrosion current density (Figure 6 (a)), concerning the anodic branches Figure 6 (b), the increase of the temperature affects the anodic branches by a passivation stage presence from -0.450 to -0.257 V/Ag/AgCl according to different temperatures. This is due to the formation of a protective inhibitive film on metal surface. The electrochemical parameters deduced from the anodic and cathodic polarization curves of MS in 0.5M H_2SO_4 without and with 2000 ppm AAE+10^{-3} M KI at different temperatures as well as the calculated inhibition efficiencies are grouped in Table 3.

According to Table 3, temperature increase from 298 to 328 K, without inhibitor, increases 10 mV the corrosion potential and the 10 times the current density, while in synergy's presence 2000 ppm AAE+ 10^{-3} M KI, it reduces 8 mV the corrosion potential and raises only 4 times current's density. In comparison, the current density values obtained, without and with the synergy (2000 ppm AAE + 10^{-3} M KI) at the same temperature, a sharp decrease of this latter up to 19 times at 328 K.

Calculated inhibition efficiency decreases at 308K, and increases from 318 K to 328 K. AAE inhibitor adsorption at 2000 ppm AAE with 10^{-3} M KI, may be physically adsorbed (weak bonds) between 298 and 308 K, and chemisorbed (strong bonds) between 318 and 328 K [6, 20].

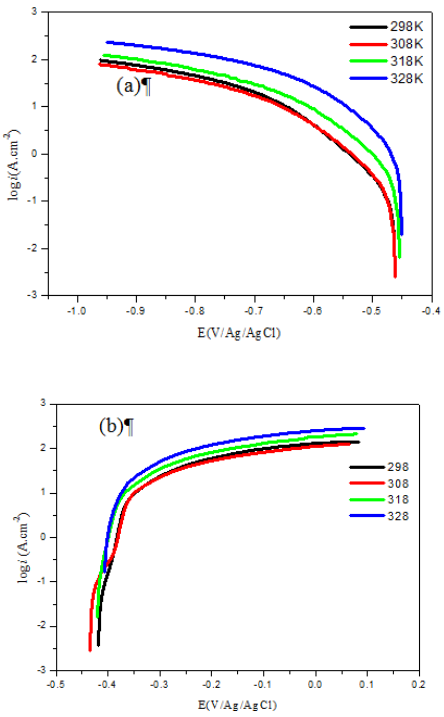

Figure 5: Cathodic (a) and anodic (b) polarization curves of MS in 0.5 M H_2SO_4 at different temperatures

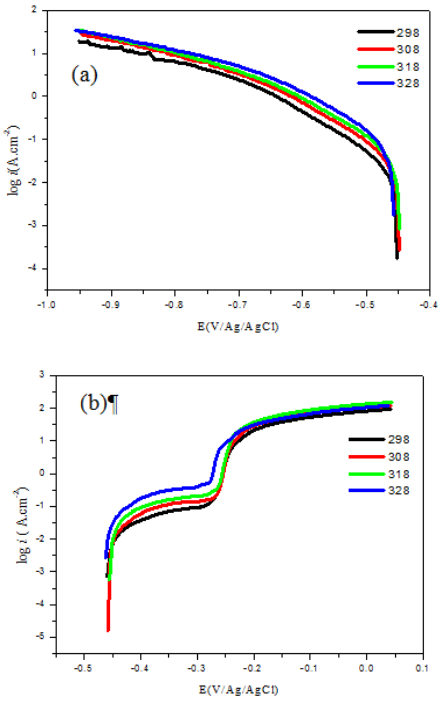

Figure 6: Cathodic (a) and anodic (b) polarization curves of MS in 0.5 M H_2SO_4 in presence of 2000 ppm AAE + 10^{-3} M KI at different temperatures

3.5.2 Thermodynamic parameters

The activation energy value is calculated according to the Arrhenius equation:

$$\log i_{corr} = -\frac{E_a}{2.303RT} + \log A \qquad \text{(E4)}$$

Where i_{corr} corrosion current density (µA.cm^{-2}); A Arrhenius constant; E_a activation energy (kJ.mol^{-1}); R perfect gas constant (J.mol^{-1}.K^{-1}); T absolute temperature (K).

The function log i_{corr}=f (1/T) shown in Figure 7, gives us two straight Arrhenius the first without synergy, and the second with it.

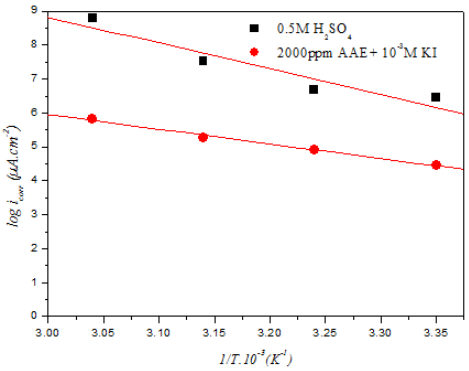

Figure 7: Arrhenius Straight lines log i_{corr} versus 1/T of MS in 0.5 M H_2SO_4 without and with 2000ppm AAE + 10^{-3} M KI

It is seen from the Table 4, the corrosion mechanism occurring with (2000 ppm AAE + 10^{-3} M KI) is characterized by an activation energy whose value is lower than that obtained in its absence .According to O. Rodovici [21], Ea value obtained without inhibitor is higher than those obtained with inhibitor, their inhibition efficiencies raise when the temperature increases which is considered as a chemisorption mechanism's characteristic.

A second representation of the Arrhenius equation allows the determination of the ΔH_a° enthalpy and the activation entropy ΔS_a°:

$$\log i_{corr} = [(\log(\frac{R}{Nh})+(\frac{\Delta S^\circ}{2.303R}))]-\frac{\Delta H^\circ}{2.303RT} \quad (E5)$$

Where i_{corr} corrosion current density (µA/cm^2); R perfect gases' constant (J.mol^{-1}.K^{-1}); T temperature (K); h Planck constant (6.626176×10^{-34}J.s); N Avogadro Number (6.02252×10^{23}); ΔH_a Activation Enthalpy; ΔS_a: Activation Entropy.

Figure 8 illustrates the variation of the ln $\left(\frac{i_{corr}}{T}\right)$ versus 1/T in 0.5M H_2SO_4 without and with 2000ppm AAE+10^{-3} M KI. The obtained straight lines have a slope equal to $\left(-\frac{\Delta H^\circ a}{R}\right)$ and an ordinate initially equal to $\left(log\frac{R}{Nh}+\frac{\Delta S^\circ a}{R}\right)$. The ΔHa and ΔS_a calculated values are grouped in Table 4.

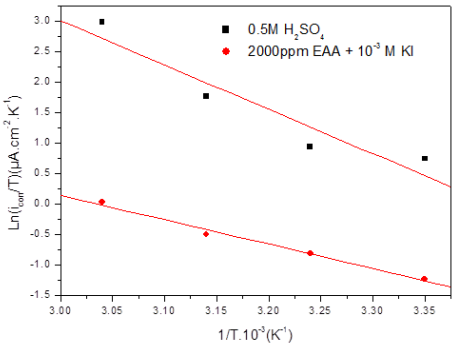

Figure 8: Arrhenius Straight lines ln (i_{corr}/*T*) versus *1/T* of MS in 0.5 M H_2SO_4 without and with 2000 ppm AAE+10^{-3} M KI

It is obvious from the Table 4 the presence of (2000 ppm AAE + 10^{-3} M KI) increases ΔH_a° and ΔS_a° which are negative, indicating respectively that the reaction is exothermic, and the negative value of ΔS_a° means on the one hand that 2000 ppm AAE + 10^{-3} M KI slowed steel dissolution in the solution (0.5 M H_2SO_4) and on the other hand, the synergy slowed down considerably the system disorder, leading to an increase of the inhibitory efficiency [16, 22].

ATR-FTIR analysis

The adsorption of inhibitor molecules on the surface of the mild steel samples was also investigated using the FTIR-ATR spectroscopy [23]. The composition of *Agave americana* extract as well as the adsorbed inhibitive film on steel surface after 1 hour immersion without and with 2000 ppm AAE alone and the synergy of 2000 ppm AAE + 10^{-3} M KI are shown in Figure 9.

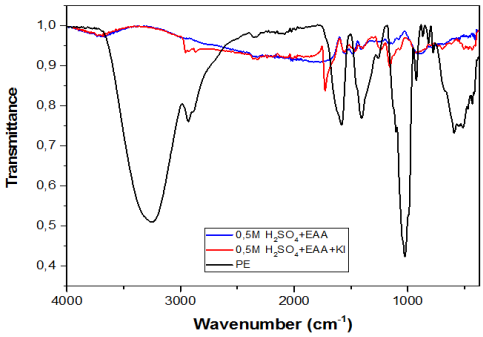

Figure 9: FT-IR spectra of AAE (a) (Black) adsorbed inhibitor film after 1h immersion in 0.5 M H_2SO_4+ 2000 ppm AAE (b) (Blue) inhibitory film adsorbed after 1h immersion in 0.5 M H_2SO_4 + 2000 ppm AAE+10^{-3} M KI (Red) (c).

From Figure 9 (a), representing the AAE spectrum, it can be noticed an adsorption's wide band at 3243.28 cm^{-1} could be attributed to the OH group a peak at 1026.13 cm^{-1} indicating C-N stretching often over lapped by others which may be a C-O-H bond or a C-O alcohol bond, a peak at 1583.01 cm^{-1}

due to the presence of an aromatic C=C, and a peak at 593cm^{-1} corresponding to C-H stretching's vibration.

In comparison of Figure 9. (a) and 9.(b), it can be observed that peak intensities' decrease denoting that there is an AAE adsorption interaction on steel surface and hence causes certain peaks shiftings towards higher frequencies' areas. As well as the O-H stretching that shifted from 3243.28 to 3668.38 cm^{-1}, showing the coordination of the inhibitor with Fe^{+2}, and peak's apparition at 1771.73 cm^{-1} attributed to C= O elongation and finally the displacement of C-H ranging from 593 to 905 cm^{-1}. Figure 9. (c), demonstrates an adsorption band at 1727.57 cm^{-1} thanks to C=O elongation of an aldehyde. The peak shift observed in the FTIR analysis confirms the interaction between AAE and the MS surface [23, 24].

3.6. Scanning electron microscopy micrographs

Figure 10. (a), shows a smooth surface. After 1 h of immersion in 0.5M H_2SO_4 (Figure 10.(b)), steel surface's attack by bites formation, in presence of AAE (Figure 10.(c)) the absence of pitting and the adsorbed film's formation on steel surface can be observed, in comparison with the micrograph (Figure 10.(d)), obtained by the synergy of 2000ppm AAE + 10^{-3}M KI, steel surface is entirely covered with a protective film indicating an improved protection with KI. Similar observations have been reported in the literature [25-27].

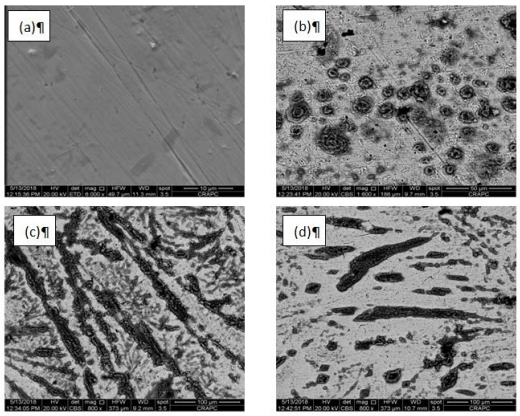

Figure 10: Micrographs (SEM) of the MS surface (a) after 1 hour immersion in 0.5M H_2SO_4(b),in 0.5M H_2SO_4+2000ppm AAE (c) in 0.5M H_2SO_4+2000ppm AAE+10^{-3}M

Table1: Electrochemical parameters deduced from steel impedance diagrams in 0.5 M H_2SO_4 without and with AAE, KI and their synergy

Parameters/Media	Rs ($\Omega.cm^2$)	CPE_{dl} ($\mu F.cm^2$)	n_1	Rp ($\Omega.cm^2$)	L (H)	R_L ($\Omega.cm^2$)	E (%)
0.5M H_2SO_4	2.42	250	0.88	159	35.07	18.42	/
0.5M H_2SO_4 +10^{-3}M KI	3.12	129	0.88	416	/		61.77
0.5M H_2SO_4 +2000ppm AAE	2.40	102	0.85	679	/		76.58
0.5M H_2SO_4 +2000ppmAAE+ 10^{-3}M KI	2.09	63	0.88	877	/		81.87

Table 2: Electrochemical parameters deduced from the polarization curves, synergy parameter and calculated inhibition efficiencies

Parameters/Media	E_{corr} ($mV_{/Ag/AgCl}$)	i_{corr} ($\mu A.cm^{-2}$)	-bc ($mV.dec^{-1}$)	E (%)	S
0.5M H_2SO_4	-461.7	628.70	95.78	/	/
0.5M H_2SO_4 +10^{-3}M KI	-462.5	194.00	101.8	69.14	/
0.5M H_2SO_4 +2000ppm AAE	-443.4	114.00	104.00	81.87	/
0.5M H_2SO_4 +2000ppm AAE+ 10^{-3}M KI	-449.6	86.53	100.3	86.24	0.40

Table 3: Electrochemical parameters deduced from anodic and cathodic polarization curves of MS in 0.5M H_2SO_4 without and with 2000ppm AAE + 10^{-3} M KI at different temperatures as well as calculated inhibition efficiencies

Parameters/Media	E_{corr} ($mV_{/Ag/AgCl}$)	i_{corr} ($\mu A.cm^{-2}$)	-bc ($mV.dec^{-1}$)	E (%)
0.5M H_2SO_4 at 298K	-461.7	628.70	95.78	-
0.5M H_2SO_4 at 308K	-462.4	790.20	102.70	-
0.5M H_2SO_4 at 318K	-455.2	1861.00	111.50	-
0.5M H_2SO_4 at 328K	-450.8	6514.00	119.00	-
0.5M H_2SO_4 +2000ppm AAE + 10^{-3}M KI at 298K	-449.6	86.53	100.30	86.24

0.5M H_2SO_4 +2000ppm AAE + 10^{-3}M KI at 308K	-448.0	137.00	114.40	82.66
0.5M H_2SO_4 +2000ppm AAE + 10^{-3}M KI at 318K	-448.7	192.60	118.10	89.65
0.5M H_2SO_4 +2000ppm AAE + 10^{-3}M KI at 328K	-457.5	339.80	121.40	94.78

Table 4: Calculated values of kinetic thermodynamic parameters for mild steel corrosion in 0.5 M H_2SO_4 in the absence and presence of 2000ppm AAE+ 10^{-3} M KI

Media/Thermodynamics parameters	**0.5 M H_2SO_4**	**2000 ppm AAE+ 10^{-3} M KI**
Ea($kJ.mol^{-1}$)	63.03	35.82
$\Delta H°_a$($J.mol^{-1}$)	-206.30	-100.85
$\Delta S°_a$($J.mol^{-1}$)	-257.98	-230.61

Conclusions

- The synergistic effect of 2000 ppm AAE +10^{-3} M KI increased the inhibition efficiency from 81.87 to 86.24% at 298 K.
- The rise in temperature until 328 K increased the inhibition efficiency to 94.78 % with KI addition.
- The calculated synergy parameter is lower at the unit indicating a competitive adsorption.
- Steel surface is negatively charged, allowing the direct adsorption of protonated water molecules and AAE cations electrostatically on metal surface.
- The obtained value from the activation energy with inhibitor is lower than that without inhibitor, which can be attributed to AAE chemisorption on steel surface.
- The adsorption reaction is exothermic.

References

[1] A. A. Farag and M .A. Hegazy. (2013). Synergistic inhibition effect of potassium iodide and novel Schiff bases on X65 steel corrosion in 0.5 M H_2SO_4. Corrosion Science. 74:168-77.

[2] B. Qian, J. Wang, M. Zheng, B. Hou. (2013). Synergistic effect of polyaspartic acid and iodide ion on corrosion inhibition of mild steel in H_2SO_4. Corrosion Science. 75:184-92.

[3] S.Ouchenane, S. Abderrahmane, A. Himour, L. Djeffal , A. Seddik. (2009). Synergistic effects of ion yttrium Y^{3+} and HEDP on mild steel corrosion resistance in 0.5 M NaCl solution. Sensor Letters. 7:937-41.

[4] G. Bahlakeh, M. Ramezanzadeh and B. Ramezanzadeh. (2017). Experimental and theoretical studies of the synergistic inhibition effects between the plant leaves extract (PLE) and zinc salt (ZS) in corrosion control of carbon steel in chloride solution. Journal of Molecular Liquids. 248: 854-70.

[5] A. Sedik, S. Abderrahmane, A. Himour. (2011). Cysteine inhibitor effects on copper corrosion in 1 M HNO_3 solution. Sensor Letters. 9: 2219-22.

[6] K. Orubite Okorosaye, I.R. Jack, M. Ochei, O. Akaranta. (2007). Synergistic effect of potassium iodide on corrosion inhibition of mild steel in HCl medium by extracts of *Nypa fruticans'* Wurmb. Journal of Applied Sciences and Environmental Management. 11(2): 27-31.

[7] I.B. Obot, S.A. Umoren, N.O. Obi-Egbedi. (2011). Corrosion inhibition and adsorption behaviour for aluminuim by extract of *Aningeria robusta* in HCl solution Synergistic effect of iodide ions. Journal of Materials and Environmental Science. 2(1): 60-71.

[8] M.Jokar, T.S Farahani, B.Ramezanzadeh. (2016). Electrochemical and surface characterizations of *morus alba pendula* leaves extract MAPLE as a green corrosion inhibitor for steel in 1 M HCl. Journal of the Taiwan Institute of Chemical Engineers. 63: 436-52.

[9] S. A. Umoren, E .E Ebenso, Studies of the anti-corrosive effect of *Raphia hookeri* exudate gum halide mixtures for aluminium corrosion in acidic medium. (2008). Pigment and Resin Technology. 37(3): 173-182.

[10] A. Khamis, M.M. Saleh, M.I.Awad. (2013). Synergistic inhibitor effect of cetylpyridinium chloride and other halides on the corrosion of mild steel in 0.5 M H_2SO_4. Corrosion Science. 66:343-49.

[11] E.E. Ebenso, H. Alemu, S.A. Umoren, I.B. Obot. (2008). Inhibition of mild steel corrosion in sulphuric acid using alizarin yellow GG dye and synergistic iodide additive. Int. J. Electrochem. Sci. 3 :1325–1339.

[12] Sameh, A., Sihem, A., Fadila, B., & Gülfeza, K. (2018). A study of the effect of *Agave Americana* extract inhibitor on the corrosion of mild steel in 0.5 M H_2SO_4. Materials Research Express. 6(1): 016504.

[13] SINGH, Priyanka, CHAUHAN, D. S., CHAUHAN, S. S., et al. (2020). Bioinspired synergistic formulation from dihydropyrimdinones

and iodide ions for corrosion inhibition of carbon steel in sulphuric acid. Journal of Molecular Liquids. 298: 112051.

[14] USMAN, Bashir J., UMOREN, Saviour A., et GASEM, Zuhair M. (2017). Inhibition of API 5L X60 steel corrosion in CO_2-saturated 3.5% NaCl solution by tannic acid and synergistic effect of KI additive. Journal of Molecular Liquids. 237:146-156.

[15] CAO, Shuyun, LIU, Dan, DING, Hui, et al. (2019). Corrosion inhibition effects of a novel ionic liquid with and without potassium iodide for carbon steel in 0.5 M HCl solution: An experimental study and theoretical calculation. Journal of Molecular Liquids. 275: 729-740.

[16] M.M.Solomon, S.A.Umoren. (2015). Enhanced corrosion inhibition effect of polypropylene glycol in the presence of iodide ions at mild steel/sulphuric acid interface, Journal of Environmental Chemical Engineering. 3:1812-26.

[17] AQUINO-TORRES, Eliazar, CAMACHO-MENDOZA, Rosa L., GUTIÉRREZ, Evelin, et al. (2020). The influence of iodide in corrosion inhibition by organic compounds on carbon steel: Theoretical and experimental studies. Applied Surface Science. 145928.

[18] R. Fuchs-Godec, Colloids Surf A.(2006). Physicochem Eng Aspects. 280: 130.

[19] H.G. Alvim, E.N. da Silva Junior, B.A. Neto. (2014). Rsc Advances. 4:54282 -54299.

[20] Solmaz, R. (2014). Investigation of corrosion inhibition mechanism and stability of Vitamin B1 on mild steel in 0.5 M HCl solution. Corrosion Science. 81:75-84.

[21] O. Radovici. (1965). Proceedings of the 2nd European Symposium on Corrosion Inhibition, Ferrara. 178.

[22] E.A. Noor. (2007). Temperature effects on the corrosion inhibition of mild steel in acidic solutions by aqueous extract of fenugreek leaves. International Journal of Electrochemical Science. 2:12.

[23] Srivastava, V., Chauhan, D. S., Joshi, P. G., Maruthapandian, V., Sorour, A. A., and Quraishi, M. A. (2018). PEG-Functionalized Chitosan: A Biological Macromolecule as a Novel Corrosion Inhibitor. ChemistrySelect. 3(7): 1990-1998.

[24] Baig, N., Chauhan, D. S., Saleh, T. A., & Quraishi, M. A. (2019). Diethylenetriamine functionalized graphene oxide as a novel corrosion inhibitor for mild steel in hydrochloric acid solutions. New Journal of Chemistry. 43(5): 2328-2337.

[25] El-Hajjaji, F., Messali, M., Aljuhani, A., Aouad, M. R., Hammouti, B., Belghiti, M. E., and Quraishi, M. A. (2018). Pyridazinium-based ionic liquids as novel and green corrosion inhibitors of carbon steel in acid medium: electrochemical and molecular dynamics simulation studies. Journal of Molecular Liquids. 249. 997-1008.

[26] H. Vashisht, I. Bahadur, S. Kumar, M. S. Goyal, G. Kaur, G. Singh, E.E. Ebenso, (2016). Synergistic interactions between tetra butyl phosphonium hydroxide and iodide ions on the mild steel surface for corrosion inhibition in acidic medium. Journal of Molecular Liquids. 224:19-29.

[27] Singh, P., Chauhan, D. S., Srivastava, K., Srivastava, V., & Quraishi, M. A. (2017). Expired atorvastatin drug as corrosion inhibitor for mild steel in hydrochloric acid solution. International Journal of Industrial Chemistry. 8(4):363-372.